Spectrum - Aplicações Operacionais Áreas de Defesa

Journal homepage: https://spectrum.ita.br

Electronic Warfare and Remote Sensing: Photonic Technology in RF Systems

High Sensitivity Long Pulse Envelope Detector Assisted by Microwave Photonics

André P. Gonçalves[1], Felipe S. Ivo[2], Olympio L. Coutinho[2]

[1] Brazilian Navy Acoustic and Electronic Warfare Center (CGAEM), Niterói/RJ - Brazil

[2] Technological Institute of Aeronautics (ITA), São José dos Campos/SP – Brazil

Article Info

Article History:

Received	25 July	2024
Revised	28 August	2024
Accepted	09 September	2024
Available online	22 October	2024

Keywords:

Envelope detection
Long pulse
High sensitivity
Microwave photonics

E-mail adresses:

andrepg43@yahoo.com.br (A.P. Gonçalves),
fivo@ita.br (F.S. Ivo),
olympio@ita.br (O.L. Coutinho).

Abstract

This article presents a concept of a long pulse envelope detector (ED) with a high sensitivity value based on Microwave Photonics (MWP). The process of envelope detecting of RF signals is achieved by the translation of the RF spectrum to the optical spectrum range followed by optical filtering to cut the lower sideband and the carrier, finally beating the remaining upper sideband into a low-speed photodetector (LSPD). The LSPD output signal is amplified by transimpedance gain. This approach depends only on the RF passing band of the phase modulator (PM) and the optical filter transfer function. This concept is experimentally demonstrated reaching envelope detector tangential signal sensitivity (TSS) values around to -40 dBm for RF input frequency range from 10 GHz to 20 GHz. The proposed architecture does not use any optical or video signal amplifier. The implementation of this approach is simple, employs few components, and Commercial off-the-Shelf (COTS).

I. INTRODUCTION

With the advent of the great development of satellite link communications and cellular telephony, the electromagnetic environment has become very dense near large urban centers. Such a fact brings a huge difficulty for electronic warfare (EW) sensors employed near urban centers[1]. With the dense electromagnetic environment, the receivers have a lot of problems separating the signals of interest from the others. When the signals of interest become those from radars with a low probability of interception (LPI) this difficulty is aggravated thanks to their low signal-to-noise ratio in the electronic warfare receiver and their large pulse width [2], [3]. When the large signal-to-noise ratio signals with smaller pulse lengths arrive at the same time as signals from radars with LPI characteristics, electronic warfare receivers have big difficulty detecting and separating these two types of signals. Electronic warfare system designers have been seeking to solve the problem of detecting radar signals with LPI characteristics by increasing the sensitivity of receivers and employing fast devices to be able to differentiate between signals incident at the same time on EW receivers, especially those of long duration [2], [3].

Techniques employed to solve the problem of overlapping long-duration and low SNR signals have been based on digital signal processing (DSP) of microwave signals, but performance is still limited due to the low sampling speed relative to the frequency bands required in modern radars [4].

An alternative approach to the problem is MWP. This is an area of human knowledge that emerged in the 1970s and employs optical energy to generate, transmits, and process RF signals [5]. The MWP aims to overcome some limitations suffered by electronics in terms of RF bandwidth, larger RF carriers, volume, weight, power consumption, and response speed [5].

The purpose of this paper is to point out the possibilities and limitations of using MWP to solve the problem of detecting signals with low SNR and overlapping long signals with short signals in duration.

II. SYSTEM CONFIGURATION AND PRINCIPLE

The principle of operating the fully photonic envelope detector is shown in Fig. 1. The laser lightwave is coupled to the phase modulator and undergoes optical phase modulation by the RF signal. The modulated optical signal passes through an optical filter. The theoretical carrier and the lower sideband of the modulated signal are rejected. The upper sideband portion of the modulated optic signal is transmitted through the filter to the photodetector, to be converted into a baseband electrical signal by direct detection. This process is similar to the one used on [6], where the authors presented this structure as a down converter for Ultra-Wideband (UWB) receiver.

There are two important processes to consider in the proper operation of this system. The first is the conversion of the phase to intensity optic modulation. The optical phase-modulated has an optical carrier and lower sideband filtered, only the upper sideband coupled to the photodetector. Fig. 2 illustrates how this filtering is done. The most common process is the use of an optical filter to eliminate one of the lateral sidebands of the modulated signal and inject the optical carrier and the remaining sideband into the photodetector [7]. The second process is self-homodyne detection. The upper sideband frequency components beating themselves. If an LSPD is chosen, it works like a low pass filter, because the RF output response is low frequency and its equivalent circuit is a current source with load in parallel junction capacitance, like Fig.1. The result of this process is the detection of the RF pulse envelope. The LSPD equivalent circuit behavior allows transimpedance gain in the output signal.

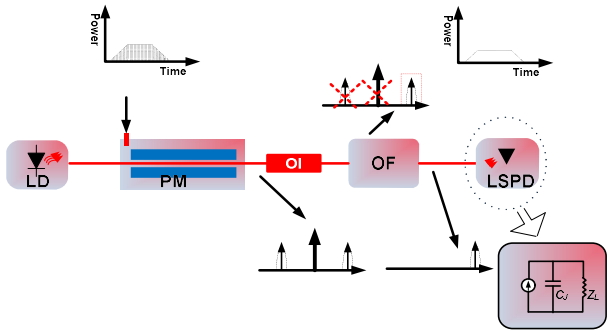

Fig. 1. Schematic diagram of the photonic ED. LD – Laser Diode, PM – Phase Modulator, OI – Optical Isolator, OF – Optical Filter, LSPD – Low-Speed Photodetector, C_J – Junction Capacitance, and Z_L - Output Load.

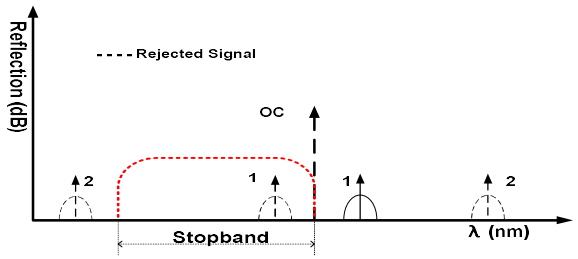

Fig. 2. Schematic diagram of the behavior of the optical filter and the optical carrier tuning. OC – Optical Carrier; 1 and 2 mean the sidebands of the optical signal modulated at the optical filter.

A. *Mathematical Modeling of the Photonic ED*

An optical electric field of laser carrier can be expressed by

$$E(t)_O = E_O exp[j(\omega_O t + \varphi_i)], \tag{1}$$

where E_O is the electric field amplitude of the signal coming from the laser diode, ω_O is the angular frequency, and φ_i is the phase. To facilitate the analysis of the electric field $E(t)_O$, the phase $\varphi_i = 0$ is considered.

Let consider an electrical RF signal feeding the RF input of a phase modulator defined as:

$$V(t)_{RF} = V[\cos([\omega_{RF} + \Delta\omega_{RF}]t + \varphi_{RF}) + \cos([\omega_{RF} - \Delta\omega_{RF}]t + \varphi_{RF})], \tag{2}$$

where V is the amplitude of the incident RF voltage, ω_{RF} is the angular frequency, and φ_{RF} is RF phase. The $\Delta\omega_{RF}$ is the instantaneous RF pulse bandwidth divided by two.

In the PM, the optical carrier undergoes a phase change expressed by [7]:

$$E(t)_O = \{E_O exp[j\omega_O t] \times exp[jm\cos([\omega_{RF} + \Delta\omega_{RF}]t + \varphi_{RF})] \times exp[jm\cos([\omega_{RF} - \Delta\omega_{RF}]t + \varphi_{RF})]\}. \tag{3}$$

The modulation index m is defined as [7]:

$$m = \frac{V}{V_\pi}\pi, \tag{4}$$

where the V_π is the half-wave voltage of the phase modulator.

The PM output is described by (3) and it becomes (5) when the Jacobi-Anger is applied, considering a small RF signal operating regime, where is m<<1, and the filter transmission frequency response is described by transmission coefficient $T(\omega)$ and phase $\varphi(\omega)$. The RF filter tuning caused the optic carrier and its lower sideband elimination ($T(\omega) = 0$) as shown in Fig. 2:

$$E(t)_T \cong T(\omega)E_1 J_1(m) \times \left\{exp\left[j\left([\omega_O + \omega_{RF} + \Delta\omega_{RF}]t + \varphi_{RF} + {}^{\pi}/_{2} + \varphi(\omega)\right)\right] + exp\left[j\left([\omega_O + \omega_{RF} - \Delta\omega_{RF}]t + \varphi_{RF} + {}^{\pi}/_{2} + \varphi(\omega)\right)\right]\right\}. \tag{5}$$

The $J_1(m)$ is Bessel function of the first kind of order 1. The $T(\omega)$ and phase $\varphi(\omega)$ parameters were considered as $T(\omega) = T$ and $\varphi(\omega) = 0$ at the out of the stopband region. The optic signal described by (5) becomes (6) due to the frequency component beating at PD. The current value at PD output described by (6) is found by calculating the value of the Poynting vector module and applying some algebraic processes. The alternated current value is estimated by:

$$i(t) = 2\Re\left(TP_o J_1(m)\right)^2 \cos(2\Delta\omega_{RF} t), \tag{6}$$

were $\Re$ is the PD responsivity, and P_o is the optic power at input system, where is $P_o \sim E_0^2$. Observing (6) is possible to realize that the electric signal at the photodetector output is the baseband signal of the RF phase modulator input. The result is the envelope of the input signal converted to current at the photodetector output. Faced with this fact, this architecture can explore low-speed photodetector, that is, photodetector with output band in the baseband (a few kHz). With the signal band in the order of kHz, it becomes possible to implement transimpedance gain with the increase of the load on the device output. The PD output voltage value (V_{out}) was estimated according to (6) and Table I. The carrier frequency considered was 17 GHz and the losses values were 8.9 dB.

TABLE I. THE THEORETICAL P_{RF} VALUES.

P_{RF} (mW)	P_o (mW)	$\Re$ (W/A)	V_π (V)	Z_L (MΩ)	i (μA)	V_{out} (V)
0.59	100	1	10.5	0.5	22.9	22.9
0.01	100	1	3.5	0.5	35.0	35.0
0.001	100	1	0.35	0.5	35.0	35.0

The performance of the ED can be improved by reducing the value of Vπ, according to (6), and increasing the load impedance [6], [8], and [9]. The value of Vπ can reach 0.3 V when an electro-optical polymer modulator was used [10].

III. EXPERIMENTAL DEMONSTRATION OF THE PHOTONIC ENVELOPE DETECTOR TSS

To demonstrate and measure the TSS of the photonic envelope detector, an experiment was carried out. The schematic diagram is shown in Fig. 3. A DFB laser is used as an optical source. The phase modulator operates at frequencies up to 20 GHz. A uniform FBG was used as an optical filter followed by a 1.5 GHz low-speed photodetector. The RF signal generator is used to perform the pulse radar signal and a high-speed digital sampling oscilloscope (DSO) is used to measure the input RF modulated signal and the output video signal, that is, the envelope of the input signal.

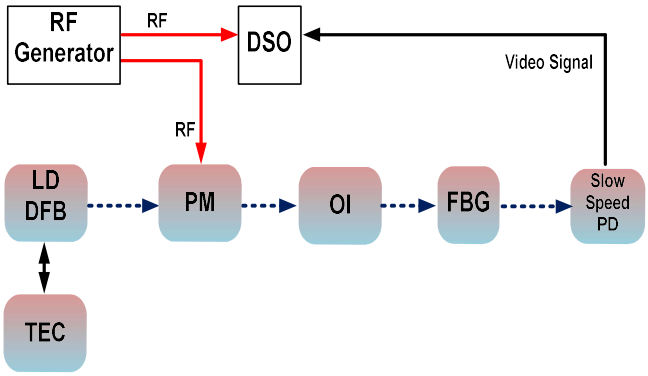

Fig. 3. Schematic diagram setup of the receiver.DFB - Distributed Feedback Laser, TEC - Thermal Electronic Cooler, PM – Phase Modulator; OI - Optical Isolator, RF - Radio Frequency, PD - Photodetector, and FBG - Fiber Bragg Grating.

The uniform optical fiber Bragg grating was chosen as an optic filter. For the sake of simplicity, Fig. 4 shows only the right side of the rejection passband optical filter, cut right on the center frequency. The right edge has a roll-off starting from the total transmission and ending at the beginning of the region's maximum optical signal reflection.

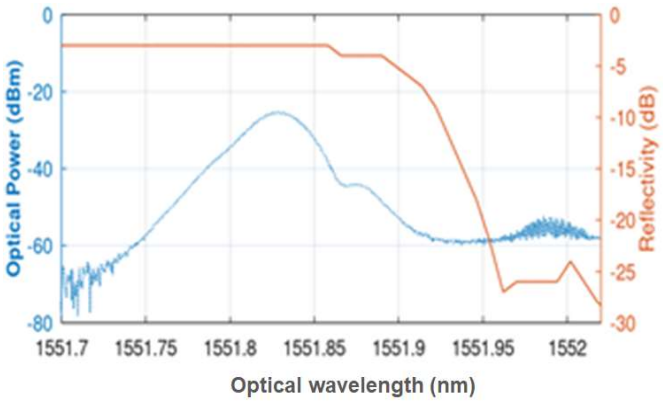

Fig. 4. The right side of the rejection passband optical filter is shown. The cut right on the center frequency is represented by an orange line. This center is around 1551.71 nm. The blue dotted line represents an optical signal modulated by an RF pulsed signal with power equal to -40 dBm.

The optical carrier and lower sideband were reduced drastically according to Fig.4. The transition region between stopband and transmission band has the roll-off around 2.86 dB/GHz according to Fig. 4. This imposes a limitation on the flatness RF response operation band, starting at 10 GHz, considering the laser carrier tuned at frequency right on the edge of the optic stopband.

The ED tuning occurs as explained previously. The TSS measuring was performed with laser tuning according presented in Fig. 4, and then applying a pulsed RF signal at the phase modulator input and varying its frequency from 0 to 20 GHz. Laser power was 100 mW and the system had 8.9 dB as optical losses. The photodetector load impedance is 500 kΩ. The minimum pulse width was 4ms and the pulse repetition interval chosen was equal to 10 ms. When the LSPD load is changed to 27 kΩ, the minimum pulse width was 25 µs and the pulse repetition interval chosen was equal to 100 µs. The RF pulses input are showed at the upper part of the figure and the baseband pulses are observed at the lower part in Fig. 5. The TSS measuring was performed by RF power variation at PM input. The RF power was decreased until the output video power signal is 8 dB above the noise level [11].

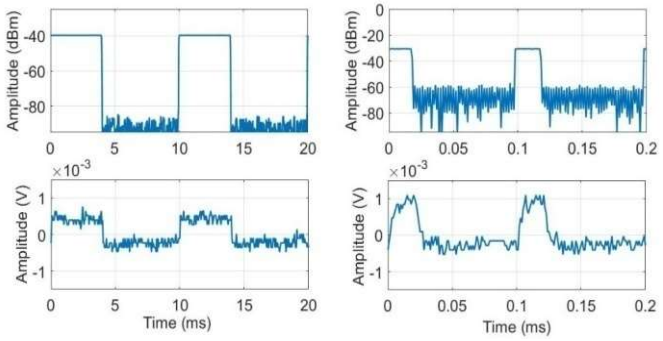

Fig. 5. The RF input signals power at 17 GHz are shown in the superior part of the figure. The pulse widths of the RF signals are 4 ms and 25 µs from the left side respectively. The lower part of the figure show video signals voltage at 8 dB condition for TSS measuring.

The RF minimum input power was -40 dBm when the LSPD load was 500 kΩ and -30 dBm when the LSPD load was 27 kΩ. When the RF signal power is set -40 dBm, it produces a modulation index equal to 9.46×10^{-4}. The TSS decreased because the transimpedance decreased. The flatness test was performed with an LSPD load equal to 500 kΩ and the RF power at PM input is equal to -40 dBm, the RF frequency value varied from 1 GHz to 20 GHz. We perceived that the TSS decreases when the pulsed signal RF frequency carrier varies from 1 GHz to 10 GHz. This fact occurs due to there is a roll-off of the Bragg grating response. If the V_π value is 0.35 V and the modulated index is 9.46×10^{-4} (the same value achieved at TSS equal to -40 dBm for V_π equal to 10,5 V @17 GHz), the TSS value will be around -69 dBm.

The video signal cut frequency depends on the load at LSPD output and the junction capacitance. When the load value is equal to 500 kΩ, the cut frequency is around 250 Hz and allows pulse width around 4 ms. The cut frequency value is around 40 kHz and pulse width is around 25 µs for load value equal to 27 kΩ. The junction capacitance value is equal for the two cases.

IV. CONCLUSIONS

This article presented a microwave photonic approach to RF envelope detection for long pulses. As this system uses an optic phase modulator, it does not need to use a bias voltage controller circuit compared with the others those use intensity modulators. The photonic envelope detector TSS reaches -40 dBm and can be around to -70 dBm for V_π value equal to 0.35 V. The flatness response of the photonic ED has decreasing values from 1 GHz to 10 GHz and flat response from 10 GHz to 20 GHz due to fiber Bragg grating roll-off. If the FBG has a roll-off better than 2.86 dB/ GHz the response to be flatter. The LSPD has an equivalent circuit composed of a current source parallel to load and junction capacitance. This circuit behaves like a low passband filter. The system can be more sensitive to long-duration pulsed signals. This fact occurs on account of the transimpedance gain; it limits the cut frequency at LSPD output. The transimpedance gain can be improved by using LSPD with junction capacitance lower than used at this approach and load increasing for the same cut frequency. This system can detect LPI signals if improved because it can present a TSS value around -70 dBm for long-duration pulses and it has short pulse filtering. The sensibility can be improved by RF pre-amplification at PM input.

ACKNOWLEDGMENTS

This work was supported by the Brazilian Air Force and the Brazilian Navy at the ITA Electronic Warfare Laboratory, as well as by the CAPES.

REFERENCES

[1] R. G. L. De Mello, F. R. de Sousa, C. Junqueira, and A. Chinatto, “Demonstrativo de um Sistema MAGE com a Antena do P-95 e Processamento em Tablet,” *Apl. Operacionais em Áreas Def.*, vol. 23, no. 1, pp. 16–21, Aug. 2022, doi: 10.55972/spectrum.v23i1.382.

[2] L. I. Ruffe and G. F. Stott, “LPI considerations for surveillance radars,” in *92 International Conference on Radar*, 1992, pp. 200–202.

[3] A. De Martino, *Introduction to modern EW systems*, 2nd ed. Artech house, 2018.

[4] P. E. Pace, *Detecting and classifying low probability of intercept radar*, 2nd ed. Artech House, 2009.

[5] J. Capmany and D. Novak, “Microwave photonics combines two worlds,” *Nature Photonics*. 2007, doi: 10.1038/nphoton.2007.89.

[6] M. Hossein-Zadeh and A. F. J. Levi, “Selfhomodyne photonic microwave receiver architecture based on linear optical modulation and filtering,” *Microw. Opt. Technol. Lett.*, vol. 50, no. 2, pp. 345–350, 2008, doi: 10.1002/mop.23065.

[7] V. J. Urick, J. D. Mckinney, and K. J. Williams, *Fundamentals of microwave photonics*. Hoboken, NJ, USA: John Wiley & Sons, Inc, 2015.

[8] R. E. and Ziemer and William H. TRANTER, *PRINCIPLES OF COMMUNICATIONS: Systems, Modulation, and Noise.* 2015.

[9] S. E. Lipsky, *Microwave passive direction finding*. SciTech Publishing, 2004.

[10] J. Liu, G. Xu, F. Liu, I. Kityk, X. Liu, and Z. Zhen, “Recent advances in polymer electro-optic modulators,” *RSC Adv.*, 2015, doi: 10.1039/c4ra13250e.

[11] M. Zahid, I. Hussain, and M. F. Iqbal, “Realistic Estimation of Signal-to-Noise Ratio in Microwave Receivers,” in *2019 16th International Bhurban Conference on Applied Sciences and Technology (IBCAST)*, 2019, pp. 952–955, doi: 10.1109/IBCAST.2019.8667117.